Kochi Chapter

Indian Geotechnical Conference
IGC 2022
15th – 17th December, 2022, Kochi

Adequacy of Stone Column Dimensions Supporting Isolated Footing when Subjected to Earthquake Loading

Priyadharshini Maniam Rajan[1][0000-0002-7374-3812] and Premalatha Krishnamurthy[2][0000-0002-5893-1495]

[1,2] Division of Soil Mechanics & Foundation Engineering, Department of Civil Engineering, College of Engineering Guindy, Anna University, Chennai, India, P.C – 600 025
Priyadharshini.civil@gmail.com
kvpremalatha@yahoo.com

Abstract. Stone columns are fundamental geotechnical units for improving soft soil deposits. It is a common application for supporting an isolated footing over stone columns when subjected to static loading. The same can also be used for earthquake loading. However, when the same element is subjected to an earthquake loading, the behaviour would not be the same. In such cases, the geometry requirement needs to be studied. The study can be done numerically using finite element analysis software, PLAXIS 3D. In this study, the earthquake of magnitude 6.9 on the behaviour of the stone column was analysed. Parametric analyses were carried out to determine the adequacy of the stone column geometry for both OSC and ESC. The parameters studied are the area replacement ratio and the encasement stiffness. The results proposed the optimum values for the area replacement ratio as 40% and 35% for earthquake loading for OSC and ESC, respectively. The optimum encasement stiffness is proposed as 1000 kN/m for static loading and stiffness greater than 2000 kN/m for earthquake loading. In this paper, the procedure for the earthquake analysis using PLAXIS 3D is described to provide better clarity to the readers.

Keywords: Stone Column, Encasement, Rigid Footing, Earthquake Analysis, PLAXIS 3D.

1 Introduction

Stone columns, a simple ground improvement technique, are commonly used to improve the site for both large and small-scale construction. The usage of ordinary and encased stone columns (OSC & ESC) has significantly increased over the last six decades [1,2,3,4]. The functional requirement of weak soil deposit for drainage [5,6] and improved strength [7,8] is fulfilled by including the stone columns. Also, the application of stone columns for liquefaction mitigation [9] is worth mentioning. Stone column usage proved to be the practical option to improve weak soil deposits. Several case studies can be found about improving such soil [10,11] subjected to static loading. When the stone columns are subjected to dynamic loadings such as earthquakes, machine foundations and explosions, the response of such composite soil site would be different. In India, the seismic zones are classified from zone II to V. Zone

II is the least affected by the earthquake, whereas zone V is the most active earthquake region [12]. There are more chances for the stone column installed site to be subjected to earthquake loading. The response of the stone columns under earthquake loading was studied and reported in the literature. However, compared to the literature on static loading, there are fewer extensive studies available on earthquake loading.

The studies on earthquakes had begun only in the past decade, particularly in areas prone to seismic activities. Kim (2012) [13] studied the site improvement by installing the stone column for the shear behaviour and response to earthquake loading using laboratory investigation of shake table tests. The earthquake loading was simulated with the Hachinohe and Northridge strong motions. In this study, the soil and the stone column behaviour was observed through the shear deformation. The site response showed that the composite ground of soil and stone columns acts as a single entity under seismic activities. Datye and Khare (2008) [14] explained the case history of a storage tank containing chemicals in Bhuj, Gujarat. The site was monitored periodically for settlement. The tank built over the stone column-treated ground had shown no signs of failure during the earthquake. Though the earthquake was of magnitude 7.7, the stone columns' ground improvement protected the structure from failure. The case study of Bhuj brings forth the importance of the stone column in mitigating failures due to seismic activities.

Guler et al. (2014) [15] numerically studied the use of geotextiles around the stone columns to prevent them from losing their integrity when subjected to earthquake loading. The 1999 Turkey earthquake was simulated to study the efficiency of the Geotextiles. Geotextiles provide better confinement to the stone column, even in very soft soils. The stone column's failure chances are exponentially high due to bulging and shearing during earthquake loading. However, the failure pattern is prevented from occurring due to the encasement.

Fernanado (2017) [16] presented a case history of a high-magnitude earthquake of 7.4 in the lands of Guatemala. The case history provides details for the site improved by the stone column through field investigations like CPT and SPT on undisturbed samples before and after the earthquake. The monitoring of the structure for settlement was performed using instrumentation. The settlement observed for the stone column improved ground before and after the earthquake was well within the permissible limit.

Reddy and Mohanty (2017) [17] presented a numerical study on stone column improved layered slope using OpenSeesPL software. The layered deposit consists of a stiff cohesive layer over a layer of saturated cohesionless soil deposit. Analyses were carried out with and without stone columns in the sloping layered deposits. Nepal earthquake of magnitude 7.8 was simulated in the software. The results have shown a considerable reduction in the peak ground parameters of the stone column compared to the unimproved ground. Sahinkaya et al. (2017) [18] studied numerically using PLAXIS 2D the effect of the diameter and length of the column, spacing between the columns, and angle of internal friction of the stone column material on the bearing capacity of the composite ground for both static and earthquake loading. Turkey's

2011 earthquake was simulated for seismic loading. The results showed that the bearing capacity of soft soils increases when subject to earthquake loading. Also, the author emphasised the efficiency of using floating columns in seismic zones.

Cengiz and Guler (2018a) [19] presented a study on the ESC and OSC through shake table laboratory tests. The dynamic loading was applied sinusoidally for two peak acceleration cases. The effect of the dynamic loading was observed in terms of the shear strain of the columns. ESCs exhibited better performance than the OSC by keeping the column intact and reducing the lateral movement of the column. Furthermore, the vertical loading on the tested columns for static and dynamic loading has shown changes in the load-carrying capacity. The dynamically loaded columns alone have lesser vertical load carrying capacity than the static ones. This reduction is more in the case of OSCs compared to ESCs. The author concluded that the OSCs are more prone to reduced strength when subjected to earthquake loading.

Cengiz and Euler (2018b) [20] proposed results based on 1g shaking table tests for OSCs and ESCs. The vertical load-carrying capacity of the ESC and OSC during and after the earthquake has shown significant behaviours. The length of the encasement also plays a crucial role, suggesting full-length encasement instead of partial encasement in seismic-prone areas. Also, the end-bearing columns performed well when compared to the floating columns under earthquake loading. The horizontal strain in the ESCs during earthquake loading depends on the encasement stiffness and the nature of the column material. On the whole, the ESCs performed better when compared to the OSCs under the action of earthquake loading.

Cengiz and Guler (2020) [21] studied the effect of the testing boundary conditions on the behaviour of the stone columns, both OSC and ESC. The free-field and rigid boundary conditions were simulated in the shaking table tests. El-Centro and Kobe earthquakes were utilised for the stone column loading schemes. In these tests, an important observation was that the encasement's major failure was observed in the vertical direction rather than the horizontal. The failure mode could be due to the seismic type of loading. Moreover, the rigid boundary condition limited the entire functioning of the encasement under seismic loading, But with the free-field condition boundary, the encasement was utterly functional and strained to the maximum horizontal strain value.

Zheng et al. (2020) [22] proposed design charts for determining the seismic bearing capacity coefficients for strip footing using the upper bound limit analysis theorem. The charts can be used to design the stone column groups in active earthquake zones. The bearing capacity factors N_{cE}, N_{qE} and $N_{\gamma E}$ for different friction angles of stone column material concerning the horizontal seismic coefficient can be obtained from the proposed design chart. Karkhush et al. (2021) [23] presented a study on the seismic behaviour of floating stone columns. In this study, the author emphasised the importance of the stone columns' length and diameter in the seismic behaviour of the composite ground. The stone column's improved soil's peak acceleration, velocity, and frequency values are much lesser than the unimproved ground. It was also reported that the variations in the deformation of short and long stone columns.

The studies from the literature emphasise the usage of stone columns to prevent the improved composite ground from failure against seismic forces. The geometrical requirement of the stone columns and the optimum value were not addressed anywhere in the literature collected so far. Therefore, this study aims to determine the adequacy of the area replacement ratio (a_r) and encasement stiffness (J_e) of the stone column supporting a rigid isolated footing when subjected to an earthquake magnitude of 6.9. The study is carried out by numerical modelling using PLAXIS 3D software.

2. Numerical modelling of stone columns supporting rigid footing using PLAXIS 3D

2.1 Numerical Modelling in PLAXIS 3D

The numerical modelling was done using the finite element modelling software PLAXIS 3D. PLAXIS 3D, with a dynamic analysis option [24], can be used to perform the earthquake analysis. The overall procedure for the analysis is similar to that of the static loading. Initially, the model dimensions were determined based on the field-scale size. Appropriate boundary conditions were decided and applied; the structural elements were added to the soil geometry; the soil and structural element properties were assigned to the respective elements; the meshing of the field-scale model; the simulation of staged construction; calculation of the numerical problem; output evaluation.

The earthquake simulation is the significant difference between the two types of analysis. For the simulation of an earthquake in a model, it is necessary to make the field-scale model to transfer the earthquake motion within the soil and the structures. The mechanism can be addressed by changing the boundary conditions. The X_{max} and X_{min} boundaries are simulated to be in the far region, so the model dimensions in the X-direction should be of greater length than the dimension of the structure analysed. The boundary assigned for the X-direction is a free-field condition. The direction normal to X has no boundary conditions, which is due to the action of the earthquake in the X-direction alone. The earthquake is applied to the field-scale model as prescribed surface displacement at the bottom of the model. The signal is given as input along with the surface displacement as a ‘dynamic multiplier’.

In this modelling, the input signal is in the form of a table using the *.smc or plain text file. SMC stands for “strong motion centre”, which can be obtained from the strong motion centre websites [25]. This study used the plain text file with time and acceleration details as the input. The input signal applied at the model’s base must travel to the soil and the structures near the ground. The boundary condition must be assigned Z_{min} as a ‘compliant base’ for the earthquake wave propagation simulation. These boundary conditions only work in the calculation stage when the interfaces are added inside the model at the boundary edges. The interfaces provide dummy node pairs for absorbing the incoming wave and carrying the incoming signal. Moreover,

the interface must not be activated in the staged construction for the earthquake analysis. The interface is used only for the creation of the node pair.

The earthquake analysis in the staged construction can be described based on the dynamic time and time steps. Dynamic time depends on the total duration of the input signal; otherwise, the time after the maximum acceleration is reached. The time steps can be obtained using Newmark implicit time integration scheme. The time step calculation itself is a critical study to be carried out. For the present analysis, the automatic time step calculation was selected. The damping ratio for the analysis was taken as a 5% benchmark value. The Rayleigh coefficients for each material were determined based on the shear wave velocity, the earthquake motion's maximum frequency, and the damping ratio. At last, the node points in the field scale model should be selected before the calculation to provide us with the curves for the vital points.

Validation of the Numerical model. The author has already validated the model using field results on the earthquake analysis [26]; the same has not been repeated here due to page restrictions.

3. Numerical modelling and Input Parameters for the field-scale model parametric analysis

The field-scale model dimensions were utilised based on the literature [26] and the need to simulate the far-field conditions for the earthquake analysis. Therefore, the model dimensions were 10 m × 5 m × 10 m (Fig. 1(a)). The depth of the model was assumed based on the homogeneous clay layer thickness of 10 m. The field problem consists of a square footing of size 5 m × 5 m supported by a group of four stone columns, and the water table was assumed to be at the footing level. The footing was modelled as a linearly elastic rigid plate element. The end-bearing stone columns were modelled as a volume element. The interfaces should be added inside the model, as shown in Fig. 1(b). The interface elements derive their properties from the adjacent soil elements.

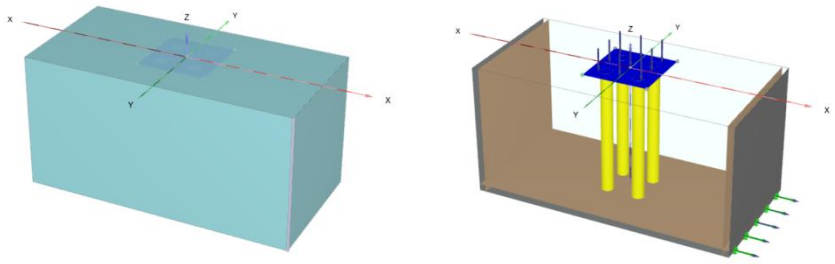

Fig. 1. Field-scale model in numerical modelling domain (a) soil profile (b) structural profile

The material model for soil and the stone column was the Mohr-Coulomb model because of its adequacy in simulating the load-settlement of stone columns. The

Mohr-Coulomb model is commonly used in most stone column problems [5,27]. For static loading conditions, the critical length for OSC and ESC was reported in the literature [27]. Nevertheless, for earthquake loading, the floating columns did not perform well [20]. So in this study, the end-bearing stone columns alone were considered. For the ESCs, the geogrid element was modelled around the stone column as a surface. The encasement stiffness was chosen based on the practical availability of the geogrid from 500 kN/m to 5000 kN/m [28].

The stone columns' diameter varied based on the a_r from 10% to 50%. It is not practically advisable to consider beyond the mentioned a_r values. Over the footing, a uniform surface load of 30 kPa was assumed. The low-intensity surface load value is the load the virgin soil can carry, which has a cohesive strength of 6 kPa [26]. The same loading was considered for comparing results with the OSC and ESC. For the prescribed surface displacement, 0.5 m was assumed [24]. The dynamic multiplier was taken from the earthquake motion of magnitude 6.9 and peak acceleration of 0.349 m/s^{2,} as shown in Fig. 2. The input signal was in the plain text file format [29]. The input parameters for the numerical analysis are tabulated in Table 1.

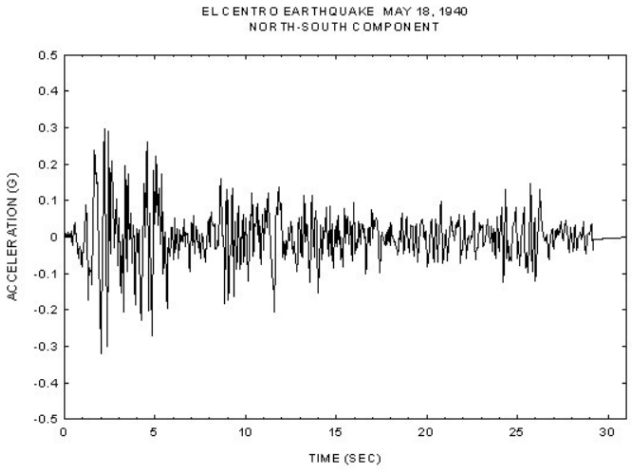

Fig. 2. Acceleration-time history of 1940 El Centro Earthquake. [29]

Table 1. Input parameters used in the numerical analysis [26]

Parameters	Soft Clay	Stone Column
Material model	Mohr-Coulomb	Mohr-Coulomb
Unit weight, γ (kN/m^3)	16	18.4
Cohesive strength, c_u (kPa)	6	0.1
Angle of internal friction, φ (°)	0	48
Young's modulus, E (kPa)	1000	10000
Poisson's ratio, ν (no unit)	0.45	0.25
Area replacement ratio, a_r (%)	-	10% - 50%
Encasement stiffness, J_e (kN/m)	-	500 – 5000

Medium size element distribution was carried out using 10-noded tetrahedral soil and stone column elements and 6-noded triangular geogrid elements. The meshing of the model is shown in Fig. 3.

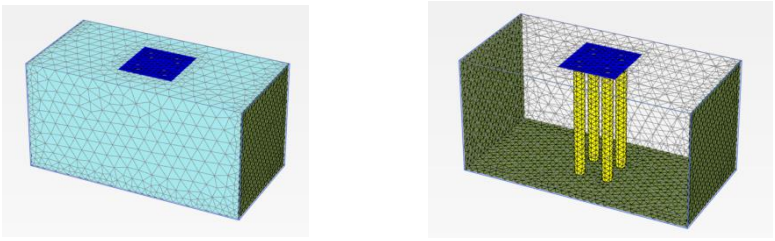

Fig. 3. Meshing of the model.

In the staged construction (Fig. 4), the initial soil stresses in the virgin state and the stone column installation were simulated in the 'initial phase' and 'phase 1', respectively. Similarly, the stone column and geogrid elements were activated 'in phases 2 & 3'. The consolidation process was simulated in phase 2. The surface loading acting on the footing and the earthquake input motion was simulated in phases 4 & 5. After planning the construction stages, the calculation points for obtaining the curves were selected. The calculation is carried out by elastic-plastic deformation analysis. The staged construction is based on the load advancement procedure; the Σ*Mstage* multiplier starts from '0' and runs up to the maximum of '1'. The output was evaluated in a separate output domain of the numerical software extracted as tables and curves—interpretations made from the results are presented in the subsequent sections.

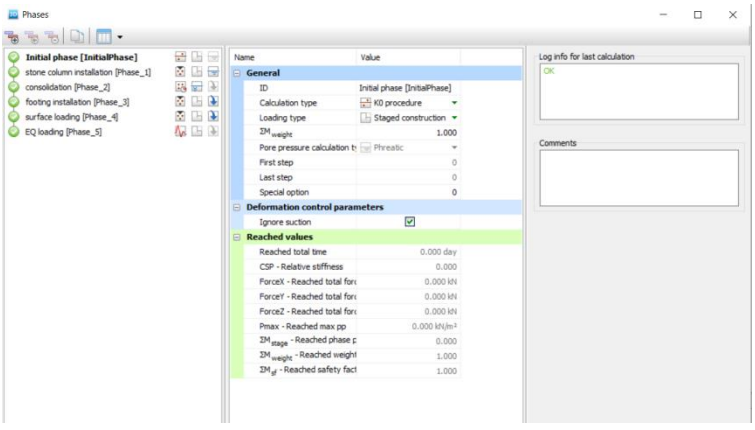

Fig. 4. Staged Construction in numerical modelling.

4. Results and Discussion

The results of the stone columns supporting rigid isolated footing subjected to earthquake loading are summarised and discussed in the following sections. The numerical analyses were carried out based on the parameters already mentioned to study the effect of the geometry of the stone column when subjected to earthquake vibrations. The soil's cohesive strength, the stone column's length, the stone column material's stiffness, and the earthquake's magnitude were all kept constant. The a_r and J_e varied from 10 % to 50% and 0 kN/m (OSC) to 5000 kN/m, respectively. The Settlement Reduction Ratio (SRR) was utilised to determine the settlement reduction profile. SRR is the settlement ratio of the improved ground to virgin soil [30]. The results determined the adequate geometry for the stone column by drawing tangential lines in the graph (Fig. 5). Also, by comparing the results from the earthquake analysis, the optimum geometry for the OSC and ESC was decided.

4.1 Effect of area replacement ratio

When the soil reinforced with OSCs and ESCs, is subjected to earthquake loading, the seismic waves affect the vertical settlement. Though there is settlement due to the static loading, the earthquake excitation would induce further disturbance and settlement of the composite ground. The variation of the settlement response of the footing on soft clay and OSC and ESC reinforced ground when subjected to the earthquake loading is shown in Fig. 5. With increasing a_r value, the SRR value reduced and became constant for an a_r value of 30% and beyond. By drawing tangent lines to the curves, the adequate value for the a_r can be obtained from Fig.5. The a_r value of 28% and 25% was observed to be adequate for the OSC and the ESC, respectively. It is observed that the a_r value influences the vertical settlement of the footing supported by the composite ground up to a particular limit. Beyond which a_r did not influence the settlement value. The constant a_r may be due to the reduction in the confinement of the stone column beyond a particular diameter. From a practical point of view, the provision of higher a_r would hinder the installation of stone columns and the provision of the encasement. Therefore from the a_r point of view for practical application, 30% and 25% would be adequate for OSC and ESC, respectively.

Effect of the encasement stiffness. The footing settlement for varying J_e and a_r are shown in Fig. 6. The OSCs settlement is shown as J_e=0 kN/m in the same figure. The earthquake's effect is also included in the settlement. It is observed that the footing settlement reduced with increased encasement stiffness. However, this reduction is only up to a stiffness value of 1000 kN/m, beyond which there is no significant settlement reduction. From the footing settlement, the effect of the encasement under earthquake loading was significant, only up to 1000 kN/m. So from this point of view, the encasement stiffness of 1000 kN/m was found adequate.

Effect of an earthquake. The earthquake acceleration in the bedrock obtained from the source was 0.349 m/s^2 [29]. When the waves reached the soil-structure, the acceleration was observed as 0.265 m/s^2 from the numerical analyses. Similarly, the acceleration values were obtained, as shown in Fig. 7. The acceleration values were observed

to reduce in the stone columns compared to the virgin soil. The reduction in acceleration would be due to the lesser vibration of waves in the denser stone column, which mitigates the amplification of the earthquake motion. Also, it can be seen from Fig. 7 that with increasing encasement stiffness of the stone column, the acceleration of the earthquake motion reduces gradually.

The divergences in the results (Fig. 7) may be due to the variation in the meshing of the numerical models. These results show that the higher the encasement stiffness, the lesser the earthquake would affect the stone column reinforced soil. Also, increasing the area replacement with stone aggregates mitigated the acceleration by 30%. The results signify the importance of the encasement and the stone columns in the earthquake-prone region. So from the acceleration values, it is proposed that the a_r can be increased up to 40%, and encasement stiffness of more than 2000 kN/m can be provided in earthquake-prone regions.

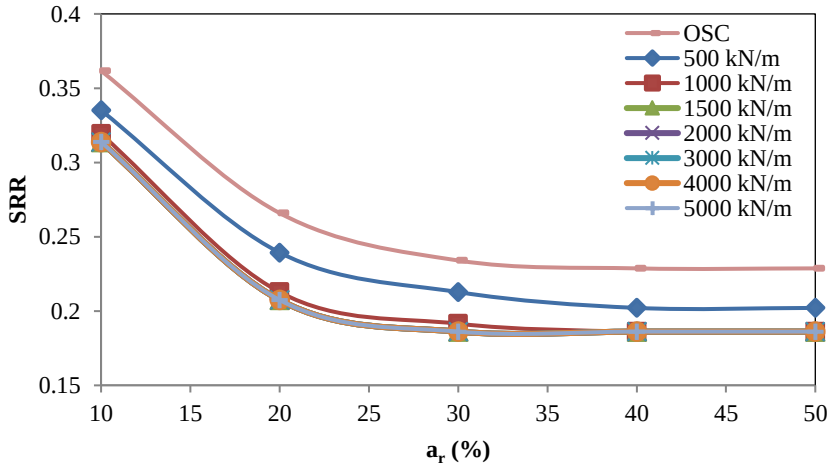

Fig. 5. Settlement Reduction Ratio for different a_r (%) and J_e (kN/m).

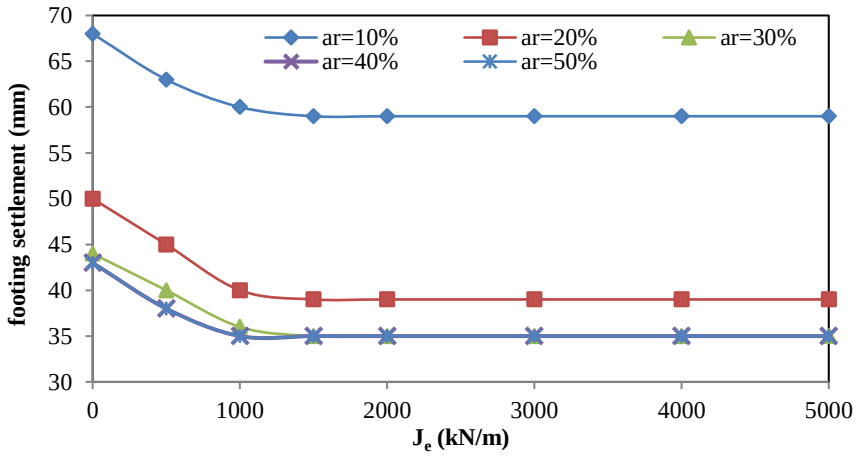

Fig. 6. Effect of J_e (kN/m) for different a_r (%).

For field application under static loading, 20% to 30% of a_r is used. It was not reported as a standard value in the literature. The optimum value of a_r of 30% for flexible footings under static loading was reported by Black et al. [31]. The current study proposes the adequate value of a_r as 30% and 25% with a 10% increment for the effect of the earthquake loading for OSC and ESC, respectively. Along with this, the encasement stiffness of 1000 kN/m was found to be adequate for static loading. However, for resisting the seismic forces, it is proposed that higher stiffness of the encasement would provide a better solution for mitigating the amplification of the seismic forces. So encasement stiffness of 2000 kN/m and above would be a better choice in earthquake-prone regions.

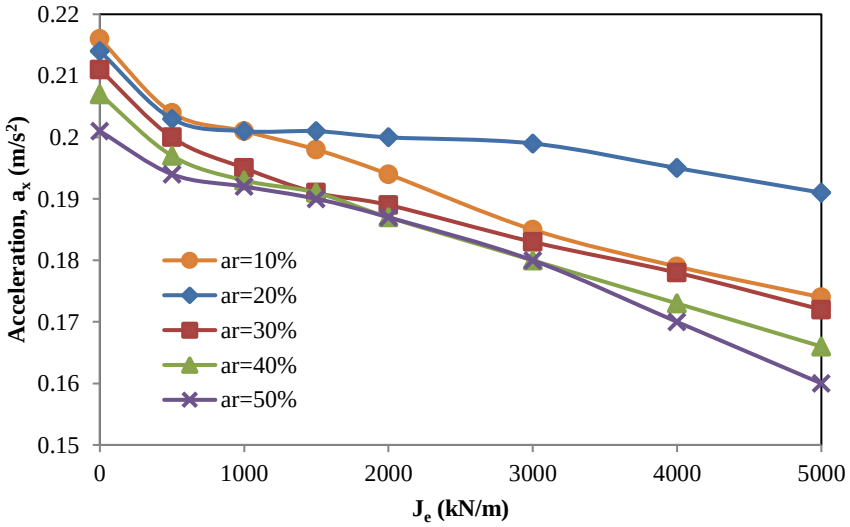

Fig. 7. Acceleration in the direction of maximum shaking for different a_r (%) and J_e (kN/m)

4.2 Stress Concentration Factor

Stress Concentration Factor (SCF) [32] denotes the ratio of the vertical stresses carried by the stone column to that of the surrounding soil. The SCF values were calculated from the numerical analysis results. The SCF values for static loading would usually be 2.5 and 5 calculated at the ground surface [32]. However, in these analyses, the SCF values range from 29 to 59. The values show that the earthquake loading has a higher effect on the stone column mechanism.

Also, it is observed (Fig. 8) that the variation of the SCF values is minimum and becomes constant for different a_r values. For 40% and 50% a_r values, the SCF values were almost constant for different encasement stiffness values. From this observation, it can be proposed that an optimum geometry is available from the stone column mechanism and agrees with the observations in the previous sections. The optimum values proposed are shown in Table 2.

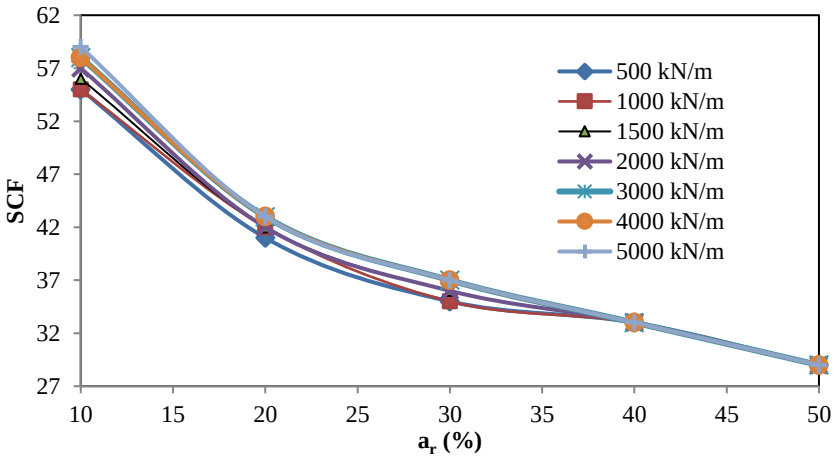

Fig. 8. Stress Concentration Factor for different a_r (%) and J_e (kN/m)

Table 2. Optimum values for OSC and ESC

Parameters	Static Loading		Earthquake Loading	
	OSC	ESC	OSC	ESC
Area replacement ratio, a_r (%)	30	25	30% + 10%	25% + 10%
Encasement stiffness, J_e (kN/m)	-	1000	-	> 2000

5 Conclusion

This paper attempts to propose optimum values for the geometry of the OSC and ESC supporting rigid isolated footing subjected to earthquake loading. A parametric analysis was carried out for varying a_r and J_e values. The results found a fair value for a_r and J_e, beyond which there is no significant effect on the footing settlement. The a_r values were found as 30% and 25% for OSC and ESC, respectively. Similarly, 1000 kN/m was found to be adequate for encasement stiffness. When the observation was made from the acceleration point of view in the direction of maximum excitation, it was found that there is a requirement for a_r and J_e values for reducing the acceleration in the soil profile. In that case, it was observed that 10% higher a_r values mitigate the amplification.

Similarly, encasement stiffness greater than 2000 kN/m serves the same requirement. Therefore, this study proposes an optimum a_r value of 40% and 35% for earthquake loading for OSC and ESC, respectively. The optimum J_e is 1000 kN/m for static loading and stiffness greater than 2000 kN/m for earthquake loading. Analyses for different magnitudes of earthquake and soil profiles would further broaden the study's scope.

References

1. Greenwood, D. A.: Mechanical Improvement of Soils below Ground Surface. In: Proceedings of Ground Engineering Conference ICE, pp. 11-22 (1970).
2. Alamgir, M., Miura, N., Poorooshasb, H.B., Madhav, M.R.: Deformation Analysis of Soft Ground Reinforced by Columnar Inclusions.Computers and Geotechnics 18(4), 267-290 (1996).
3. Priebe, H.J.: The Design of Vibro Replacement. Ground engineering 28(10), 31 (1995).
4. Black, J., Sivakumar, V., McKinley, J.D.: Performance of Clay Samples Reinforced with Vertical Granular Columns. Canadian Geotechnical Journal 44(1), 89-95 (2007).
5. Castro, J., Sagaseta, C.: Deformation and Consolidation around Encased Stone Columns. Geotextiles and Geomembranes 29(3), 268-276 (2011).
6. Rajesh, S.: Time-Dependent Behaviour of Fully and Partially Penetrated Geosynthetic Encased Stone Columns. Geosynthetics International 24(1), 60-71 (2017).
7. Hughes, J.M.O., Withers, N.J.: Reinforcing of Soil Cohesive Soil with Stone Columns. Ground Engineering 7(3), 42–49 (1974).
8. Hughes, J.M.O., Withers, N.J., Greenwood, D.A.: A Field Trial of the Reinforcing Effect of a Stone Column in Soil. Geotechnique 25(1), 31-44 (1975).
9. Asgari, A., Oliaei, M., Bagheri, M.: Numerical Simulation of Improvement of a Liquefiable Soil Layer using Stone Column and Pile-Pinning Techniques. Soil Dynamics and Earthquake Engineering 51, 77-96 (2013).
10. Datye, K.R., Nagaraju, S.S.: Design Approach and Field Control for Stone Columns. In: Proceedings of 10th International Conference on SMFE 3, pp. 637-640 (1981).
11. White, D.J., Pham, H.T., Hoevelkamp, K.K.: Support Mechanisms of Rammed Aggregate Piers I: Experimental Results. Journal of Geotechnical and Geoenvironmental Engineering 133(12), 1503-1511 (2007).
12. PIB Homepage, https://pib.gov.in/PressReleasePage.aspx? PRID=1740656, last accessed 2022/8/8.
13. Kim, J., Son, S., Mahmood, K., Ryu, J.: Site Response and Shear Behavior of Stone Column Improved Ground under Seismic Loading. In: Proceeding of the 15th Worlds Conference on Earthquake Engineering (2012).
14. Datye, K.R., Khare, M.G.: Performance of Large Storage Tank in Bhuj Earthquake. In: International Conference on Case Histories in Geotechnical Engineering, pp. 1-6. Missouri S&T, Arlington (2008).
15. Guler, E., Alexiew, D., Abbaspour, A., Koc, M.: Seismic Performance of Geosynthetic-Encased Stone Columns. Transportation Research Record, 2462(1), 77-88 (2014).
16. Callejas, F., Ronaldo, L.: Seismic ground improvement: Stone Columns Performance for a Power Plant in the Southern Alluvial Plains of Guatemala. In: Proceedings of the 19th ISSMGE, pp. 2485-2488. Seoul (2017).
17. Reddy, C.S., Mohanty, S.: Seismic Behavior of Stone Column on s Sloping Layered Soil. In: 6IYGEC2017, pp.1-4. India (2017).
18. Şahinkaya, F., Vekli, M., Çadır, C.C.: Numerical Analysis under Seismic Loads of Soils Improvement with Floating Stone Columns. Natural Hazards 88(2), 891-917 (2017).
19. Cengiz, C., Güler, E.: Seismic Behavior of Geosynthetic Encased Columns and Ordinary stone columns. Geotextiles and Geomembranes, 46(1), 40-51 (2018a).
20. Cengiz, C., Guler, E.: Shaking Table Tests on Geosynthetic Encased Columns in Soft Clay. Geotextiles and Geomembranes, 46(6), 748-758 (2018b).
21. Cengiz, C., Guler, E.: Load Bearing and Settlement Characteristics of Geosynthetic Encased Columns under Seismic Loads. Soil Dynamics and Earthquake Engineering, 136, 1-14,106244 (2020).

22. Zheng, G., Xia, B., Zhou, H., Zhao, J., Yu, X., Sun, X., Du, J.: Seismic Bearing Capacity of Strip Footings on Ground Reinforced by Stone Columns using Upper-bound Solutions. International Journal of Geomechanics, 20(9), 06020024 (2020).
23. Karkush, M.O., Jihad, A.G., Jawad, K.A., Ali, M.S. and Noman, B.J., Seismic analysis of floating stone columns in Soft Clayey Soil. In: E3S Web of Conferences, 318. 01008. EDP Sciences (2021).
24. Brinkgreve, R. B. J., Zampich, P. M., Manoj, R. N.: Plaxis CONNECT Edition V20 User Manuals. Plaxis bv, Bentley Systems, Netherlands (2019).
25. Strong-Motion Virtual Data Centre Homepage, https://www.strongmotioncenter.org/vdc/scripts/default.plx, last accessed on 2022/7/27.
26. Priyadharshini, M. R., Premalatha, K.: Deformation of Stone Column Subjected to Earthquake Loading by Numerical Analysis. In: Sitharam, T.G., Parthasarathy, C.R., Kolathayar, S. (eds.) Lecture Notes in Civil Eng., Ground Improvement Tech. pp.187-200. Springer, Singapore (2021).
27. Miranda, M., Fernández-Ruiz, J., Castro, J.: Critical length of encased stone columns. Geotextiles and Geomembranes 49(5), 1312-1323 (2021).
28. Murugesan, S., Rajagopal, K.: Geosynthetic-Encased Stone Columns: Numerical Evaluation. Geotextiles and Geomembranes, 24(6), 349-358 (2006).
29. Vibration-data Homepage, http://www.vibrationdata.com/elcentro.htm, last accessed 2022/8/8.
30. Benmebarek, S., Remadna, A., Benmebarek, N.: Numerical Modelling of Stone Column Installation Effects on Performance of Circular Footing. International Journal of Geosynthetics and Ground Engineering, 4(23), 1-15 (2018).
31. Black, J. A., Sivakumar. V., Bell, A.: The Settlement Performance of Stone Column Foundations. Geotechnique 61(11), 909–922 (2011).
32. IS:15284 (Part 1): Design and Construction for Ground Improvement - Guidelines, Stone columns. Bureau of Indian Standards, New Delhi (2003).